A99-33650

AIAA 99-3589
Streamwise Evolution of Turbulent Boundary Layers in Arbitrary Pressure Gradients

A. E. Perry, I. Marusic, M. B. Jones and S. Hafez

Department of Mechanical and Manufacturing Engineering
University of Melbourne, Parkville, Vic. 3052 Australia

30th AIAA Fluid Dynamics Conference
28 June - 1 July, 1999 / Norfolk, VA

AIAA-99-3589

STREAMWISE EVOLUTION OF TURBULENT BOUNDARY LAYERS IN ARBITRARY PRESSURE GRADIENTS

A. E. Perry, I. Marusic*, M. B. Jones and S. Hafez
Department of Mechanical and Manufacturing Engineering
University of Melbourne, Parkville, VIC 3052, AUSTRALIA

Abstract

A closure scheme is proposed for computing the evolution of turbulent boundary layers developing in arbitrary pressure gradients. Firstly the important parameters pertaining to the flow in the general non-equilibrium case are identified. Then the equations that govern the streamwise evolution of a turbulent boundary layer are formulated in terms of these parameters. This is done by using classical similarity laws such as Prandtl's law of the wall and Coles' law of the wake in conjunction with the mean continuity and integral momentum equations. Finally a closure scheme based on empirical data in conjunction with the assumption that the Reynolds shear stress profiles can be described by a two parameter family is used to predicted the evolution for several flow cases and the results compared to experiments.

1 Introduction

Perry, Marusic, and Li[1] developed a framework for computing the evolution of a turbulent boundary layer. An important feature of their closure scheme was the expression for the total shear stress profile which they found to be given by

$$\frac{\tau}{\tau_0} = f_1[\eta, \Pi, S] + g_1[\eta, \Pi, S]\zeta + g_2[\eta, \Pi, S]\beta \qquad (1)$$

where $\eta = z/\delta_c$, z is the distance normal to the wall, δ_c is the boundary layer thickness, $S = U_1/U_\tau$ where U_1 is the local freestream velocity and U_τ is the friction velocity, Π is Coles[2] wake factor, $\beta = (\delta^*/\tau_0)(dp/dx)$ is the Clauser pressure gradient parameter where δ^* is the displacement thickness, p is the freestream static pressure, τ_0 is the wall shear stress, x is streamwise distance and $\zeta = S\delta_c d\Pi/dx$. Equation (1) is derived from the mean momentum differential and continuity equations and assuming the mean velocity profile could be described by Coles[2] law of the wall, law of the wake. The functions f_1, g_1 and g_2 are known analytical functions, which can be derived with the aid of *Mathematica* or *Maple*. Hence from (1) the parameters required to describe the state of the layer are found to be;

$$\Pi, \quad S, \quad \beta \quad \text{and} \quad \zeta .$$

One important property of f_1, g_1 and g_2 is that they become independent of S as $S \to \infty$. Perry et al.[1] made use of this information along with empirical data to formulate a closure equation. However this closure equation was only applicable to flows which were either in approximate equilibrium or quasi-equilibrium. In approximate equilibrium flows, Π is assumed to be constant and the shear stress profiles are characterised only by Π (approximately) and in quasi-equilibrium flows, Π is allowed to vary with x provided the parameter ζ has a negligible effect on the shear stress profiles, ie

$$\frac{g_1[\eta, \Pi, S]\zeta}{f_1[\eta, \Pi, S] + g_2[\eta, \Pi, S]\beta} \ll 1 . \qquad (2)$$

In these restricted flow cases the closure problem reduces to considering the relation

$$C[\Pi, \beta, S] = 0 . \qquad (3)$$

Hence from data, if we know β at a given S for a fixed Π (i.e. for one experimental data point), then for this fixed Π we can find β versus S for all S using equation (1) to ensure that τ/τ_0 profiles are matched (approximately) for all S. Now, it is found that for S sufficiently large, $\beta = \beta_a$ (the asymptotic value of β) and C is no longer a function of S. If this procedure is repeated for different values of Π, a one-to-one relationship between β_a and Π can be found which is based on experiment. This formulation is consistent with a universal relation for eddy viscosity ϵ, i.e. $\epsilon/(\delta_c U_\tau) = \phi[\eta, \Pi]$. Unfortunately, such formulations are known to break down in non-equilibrium flows, i.e. flows with significant ζ con-

*Department of Aerospace Engineering and Mechanics University of Minnesota, Minneapolis, MN 55455 USA.

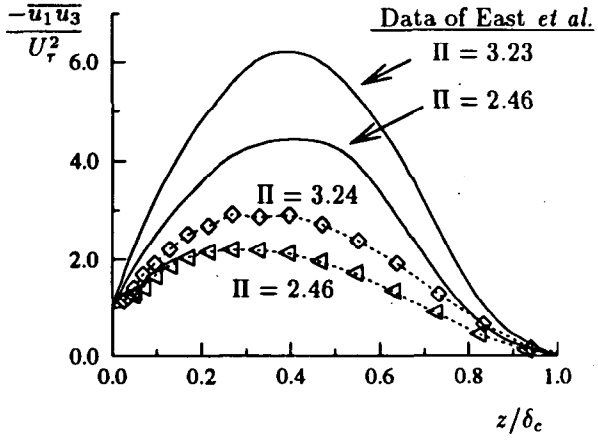

Figure 1: Comparison of nonequilibrium data of Marusic and Perry[3] where $\Pi = 2.46$ and 3.23 (10APG) with interpolated data for the same values of Π for the equilibrium flow of East et al.[5]

tribution. Figure 1, which is taken from Marusic and Perry[3], shows clearly how flows with the same Π value can have very different shear stress distributions. Furthermore the recent experimental results of Jones[4] suggest that even for quasi-equilibrium flows, neglecting ζ may not be a valid assumptions, that is while ζ may not play an important part in the momentum balance, it has a significant influence on the closure formulation.

In the recent paper Perry, Marusic, and Jones[6] the work of Perry et al.[1] was extended to include the effect of the parameter ζ, this allowed the evolution of general non-equilibrium flows to be computed. In this paper we summarise the background theory of this new method and show how it can be used to compute flows ranging from non-equilibrium flows to those approaching equilibrium.

2 New formulation

The restricted formulation of Perry et al.[1] will now be extended with the effect of the parameter ζ included so that the general non-equilibrium flow problem can be solved. Therefore, the function (3) needs to be replaced by

$$\mathcal{F}[\Pi, S, \beta, \zeta] = 0 \tag{4}$$

and so we have to work in a higher dimensional space than did Perry et al.[1]. It is assumed no further parameters are involved in (4) and $\mathcal{F}$ is universal. Hence in order to describe the state of the layer, we require three of the four variables in the above expression. The mapping out of equation (4) from experimental data would be extremely difficult because of the sparseness of the data. In what follows, a mathematical framework for interpolation and extrapolation with sparse data is developed.

From figure 1 it is obvious that the shear stress distribution needs at least two parameters to describe it and we will assume that

$$\frac{\tau}{\tau_0} = f[\eta, \Pi, \beta_a]. \tag{5}$$

For quasi-equilibrium flows Perry et al.[1] relied on a one-parameter family to describe the shear stress, i.e. $\tau/\tau_0 = f[\eta, \Pi]$ where f is assumed to be universal.

With the assumption implied in (5) and used in conjunction with (1), some information can be obtained regarding (4) as follows. Consider the $S - \beta$ plane at a fixed Π. If such a plane contains an experimental datum point D, then S, Π, β and ζ are known for that datum point and so also is τ/τ_0 versus η from (1). Trace out a curve for increasing S of fixed shear stress profile shape on the $S - \beta$ plane. By taking $S \to \infty$ we obtain asymptotic values of ζ_a and β_a as shown in figure 2. (Going to $S = \infty$ is simply a convenient curve-fitting procedure and could never be approached experimentally). This process of keeping profile shape fixed will be referred to as "profile matching" and the details of the method used here are given in the following section. If this process is repeated often enough for different Π's then we obtain a $\Pi - \beta_a$ diagram with distributions of extrapolated data points corresponding to different values of ζ_a. By a surface fit to ζ_a on the the $\Pi - \beta_a$ plane, contours of ζ_a can be mapped out and we thus have a known universal function ψ

$$\psi[\Pi, \beta_a, \zeta_a] = 0. \tag{6}$$

By shear stress profile matching we can then map out isosurfaces of ζ in $\Pi - \beta - S$ space and thus (4) is known.

2.1 Profile matching

The shear stress profile matching technique used here involves using a least squares error criterion. We find

$$\begin{aligned} \frac{\partial}{\partial \beta}\left\{\int_0^1 \left[\left(\frac{\tau}{\tau_0}\right) - \left(\frac{\tau}{\tau_0}\right)_D\right]^2 d\eta\right\} &= 0 \\ \frac{\partial}{\partial \zeta}\left\{\int_0^1 \left[\left(\frac{\tau}{\tau_0}\right) - \left(\frac{\tau}{\tau_0}\right)_D\right]^2 d\eta\right\} &= 0 \end{aligned} \tag{7}$$

where τ/τ_0 is the shear stress distribution at any point on the $\beta - S$ plane for fixed Π and $(\tau/\tau_0)_D$ is the shear stress distribution at a known datum point, e.g. point D on figure 2. For a well defined

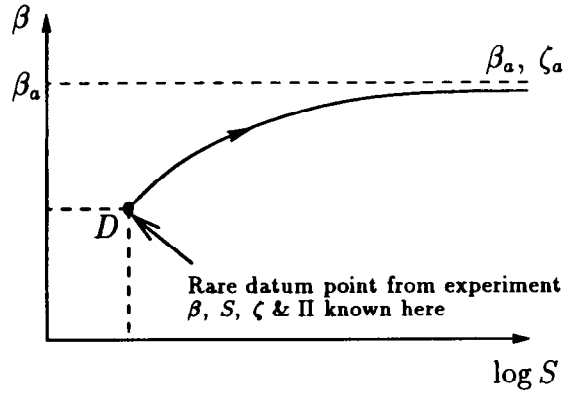

Figure 2: Solid line indicates the trajectory of least squares error in shear-stress profile matching with known profile at D. Π is fixed.

matching trajectory the solid line in figure 2 would correspond to a deep valley on a contour plot of least square error. Taking (7) to $S \to \infty$ means that we use $\partial/\partial\beta_a$ and $\partial/\partial\zeta_a$ as the derivatives and this gives

$$\begin{aligned} A_1[\Pi,S] + B_1[\Pi,S]\zeta + C_1[\Pi,S]\beta \\ = D_1[\Pi]\zeta_a + E_1[\Pi]\beta_a \\ A_2[\Pi,S] + B_2[\Pi,S]\zeta + C_2[\Pi,S]\beta \\ = D_2[\Pi]\zeta_a + E_2[\Pi]\beta_a \end{aligned} \tag{8}$$

where A_1, A_2 etc are all known analytical functions. Their functional form will depend on the type of wall-wake formulation which is chosen. Several forms have been proposed and in the Perry et al.[1] study the formulation due to Lewkowicz[7] was used. Here we will use the recently proposed formulation of Jones[4]

$$\frac{U}{U_\tau} = \overbrace{\underbrace{\frac{1}{\kappa}\ln\left[\frac{zU_\tau}{\nu}\right] + A - \frac{1}{3\kappa}\eta^3}_{\text{Pure wall flow}}}^{\text{Law of the wall}} + \overbrace{\frac{\Pi}{\kappa}2\eta^2(3-2\eta)}^{\text{Law of the wake}} \tag{9}$$

where $\kappa = 0.41$ is the Karman constant and A is the universal smooth wall constant taken here to be 5.0. This formulation was found to work particularly well in describing the "pure-wall" component of the flow as found in sink flows.

2.2 Evolution equations

The equations which govern the streamwise evolution of a turbulent boundary layer can be found after considerable algebra by using the momentum integral equation, the law of wall and law of the wake together the definitions for β and ζ. A coupled set of ODE's result; these are

$$\frac{dS}{dR_x} = \frac{\chi R[S,\Pi,\zeta,\beta]}{SE[\Pi]\exp[\kappa S]} \tag{10}$$

and

$$\frac{d\Pi}{dR_x} = \frac{\zeta\chi}{S^2E[\Pi]\exp[\kappa S]}, \tag{11}$$

where

$$R_x = \frac{xU_0}{\nu} \quad \text{and} \quad \chi = \frac{U_1}{U_0} = \chi[R_x, K]\,.$$

K is often referred to as an acceleration parameter and is defined as

$$K = \frac{\nu}{LU_0}\,. \tag{12}$$

In all of the above U_0 is the value of the freestream velocity at some initial point $R_x = 0$ or $x = 0$, U_1 is the freestream velocity at some general value of x or R_x and L is a characteristic length scale of the U_1 distribution. Equation (10) comes from the momentum integral equation and the law of wall and law of the wake and equation (11) come from the definition of ζ and the law of the wall and law of the wake. The functions appearing in (10) and (11) are defined in the Appendix.

Two auxiliary equations are needed to solve for the integration and these are equation (4), i.e.

$$\mathcal{F}[\Pi,S,\beta,\zeta] = 0$$

and

$$S^2E[\Pi]\exp[\kappa S]\frac{1}{\chi^2}\frac{d\chi}{dR_x} = -\frac{\beta}{C_1[\Pi]} \tag{13}$$

which comes from from the law of the wall, law of the wake and the definition of β. All of the above equations can be reduced to two coupled ODE's of the form

$$\frac{dS}{dR_x} = \phi_1[\Pi,S,R_x,K] \tag{14}$$

$$\frac{d\Pi}{dR_x} = \phi_2[\Pi,S,R_x,K]. \tag{15}$$

2.3 Closure equation

In order to evaluate the evolution of the boundary layer a general expression is needed for (6), i.e.

$$\psi[\Pi,\beta_a,\zeta_a] = 0.$$

Although the attached eddy model can assist us for quasi-equilibrium flow, at the present time we still require a model for finite ζ_a values. The answer can be found empirically provided enough experimental information is available. A survey of existing experimental studies showed surprisingly how little reliable data is presently available.

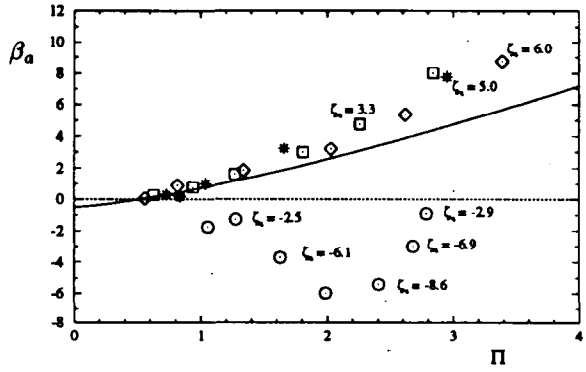

Figure 3: Available experimental data used to aid formulation of (6). Some typical values of ζ_a are shown for various data points. Data source : □ - Marusic and Perry[3] 30APG, ○ - Bradshaw and Ferriss[8], ◇ - Marusic and Perry[3] 10APG, ∗ - Samuel and Joubert[9].

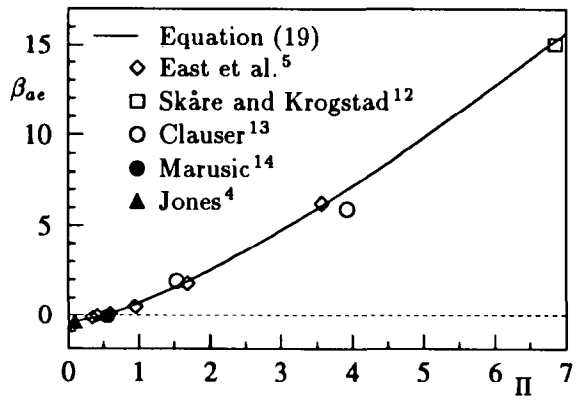

Figure 4: Experimental data which is in approximate equilibrium compared to (18). Note the experimental values of β_{ae} are determined using the shear stress matching technique given by (8).

Moreover, in many cases the data in the literature failed the two-dimensional conservation of mean momentum test using (1). A collection of available results, believed to be reliable, covering a representative range of $\Pi - \beta_a - \zeta_a$ space is shown in figure 3. This plot represents the present state of experimental knowledge of closure of turbulent boundary layers and it can be seen to be very sparse. All of this data had Reynolds shear stress data available which agreed reasonably well with equation (1). Using this data, a first tentative form for (6) has been estimated to be

$$\Delta\beta_a = \begin{cases} \zeta_a^2(1.10/\Pi^2) & \text{if } \zeta_a \geq 0 \\ \zeta_a(0.62 + 0.25\Pi) & \text{if } \zeta_a < 0 \end{cases} \quad (16)$$

Here

$$\Delta\beta_a = \beta_a - \beta_{ae} \quad (17)$$

where β_{ae} is the value of β_a for $\zeta_a = 0$, ie. equilibrium flows and it is given by

$$\beta_{ae} = -1/2 + Q\Pi^{4/3} \quad (18)$$

where Q is a universal constant. The form of (18) was derived using the attached eddy model of Perry and Marusic[10] and hence the constants $-1/2$ and $4/3$ come entirely from theory. Figure 4 shows experimental data (from approximate equilibrium flows) compared to (18) and it is seen that $Q = 1.21$ represents a good fit. Therefore

$$\beta_{ae} = -1/2 + 1.21\Pi^{4/3} \quad (19)$$

which is very close to the relationship proposed by White[11].

The resulting functional form for (6), using (16), (17) and (19) can be summarised by plotting contours of ζ_a on the $\beta_a - \Pi$ plane and this is shown in figure 5.

Given the evident sparseness of the experimental data, equation (16) can only be regarded as tentative. However, it is useful as shown in figure 5 as a means to illustrate and summarise the approach being proposed here. One interesting feature worth noting is the discontinuity of the ζ_a surface slope on the $\Delta\beta_a - \Pi$ plane at $\Delta\beta_a = 0$. This might reflect the possibility that the development and relaxation processes are quite different physically.

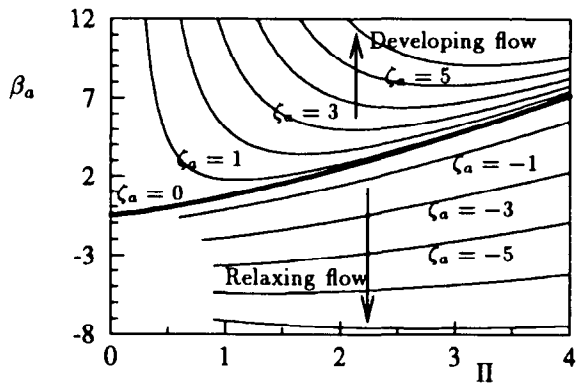

Figure 5: β_a versus Coles wake factor for different ζ_a using (16), (17) and (19).

3 Application to experiments

Equations (14) and (15) are applicable to completely general non-equilibrium turbulent boundary layer evolution and using (16) we are now in

a position to compute the boundary layer evolution. In the following two cases will be considered namely; non-autonomous and autonomous.

3.1 Non-autonomous cases

Here the independent variable R_x appears explicitly on the RHS of equations (14) and (15) making them non-autonomous. Given an initial mean velocity profile and using (16) the evolution has been calculated and the results are shown in figure 6. The flows shown in figure 6 are all non-equilibrium flows and cover a broad distribution of adverse pressure gradient conditions. The flow of Bradshaw and Ferriss[8] is a relaxing flow, the two Marusic and Perry[3] cases are developing flows as is the Samuel and Joubert[9] case. Good agreement can be seen with experiment. This should be so since the data tested was used to formulate (16) in the first place. These calculations at least show that the scheme proposed is viable and the mathematical machinery is working correctly.

3.2 Autonomous cases

For flow cases such as zero pressure gradient, source flow or sink flow, $(1/\chi^2)(d\chi/dR_x)$ in (13) becomes K, where for source flows

$$K = \frac{-2\pi\nu}{Q} = \frac{-\nu}{U_0 L},$$

for sink flows

$$K = \frac{2\pi\nu}{Q} = \frac{\nu}{U_0 L}$$

and for zero pressure gradient flows $K = 0$. Here Q is the strength of the source or sink and L is a constant (see figures 7 and 10). For these cases (14) and (15) become autonomous by an appropriate change in the independent variable R_x to T_x to give

$$\frac{dS}{dT_x} = \psi_1[\Pi, S, K] \qquad (20)$$

$$\frac{d\Pi}{dT_x} = \psi_2[\Pi, S, K]. \qquad (21)$$

where $T_x = -(\ln(1 - R_x K))/K$. Also in the limit as $K \to 0$ (ie. zero pressure gradient flow) $T_x = R_x$. This means that solution trajectories can be displayed on the $S - \Pi$ phase plane for various initial conditions, eg. S_0, Π_0 at $R_x = 0$ for fixed K.

3.2.1 Source flow

Figure 7 shows a schematic representation of source flow and calculations for a series of different initial conditions. As mentioned earlier, this is an

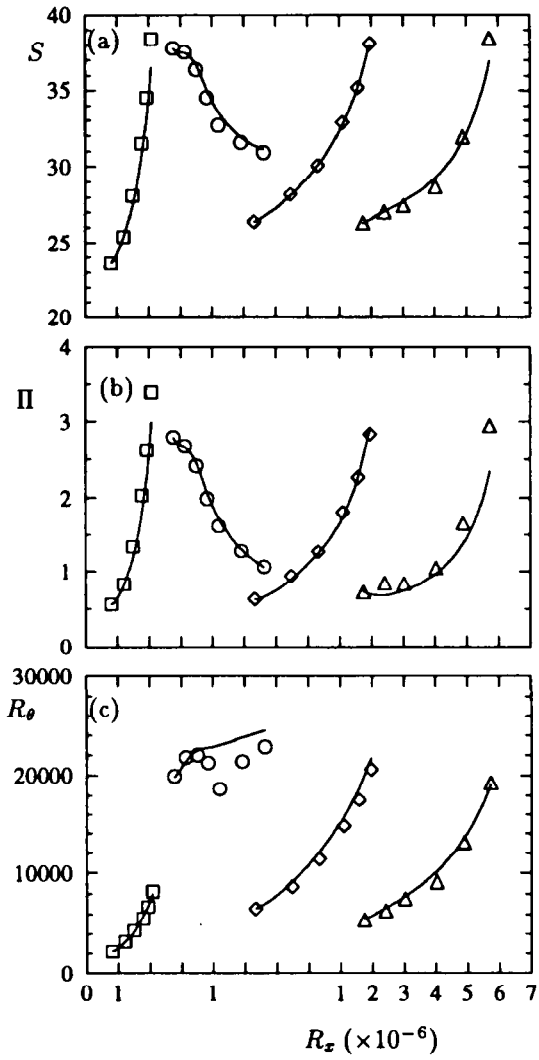

Figure 6: Nonequilibrium adverse pressure gradient data of ○ Bradshaw and Ferriss[8], relaxing flow, Marusic and Perry[3], ◇ 30APG and □ 10APG flow, and △ Samuel and Joubert[9], positively increasing APG flow. Solid lines are the corresponding computed solutions of (10) and (11) using (13), (8) and (16). Note shifts in abscissa.

autonomous system and so the solution can be displayed on a $S - \Pi$ phase plane diagram. There is no experimental data for this case so it represents a genuine prediction. The range of validity of (16) is very limited in ζ_a and this may have been exceeded in computing figure 8. The heavy broken line in figure 8 is from the Perry et al.[1] quasi-equilibrium calculation using (19) for β_{ae}. It can be seen that for this latter calculation we are not free to chose the initial conditions for Π and S independently.

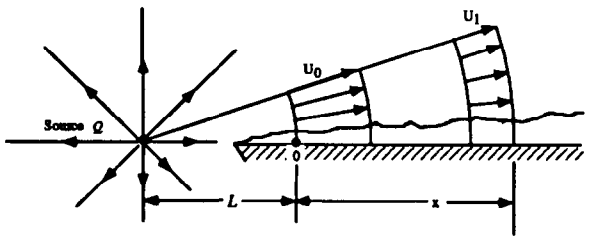

Figure 7: Schematic of source flow boundary layer, note origin for x is arbitrary.

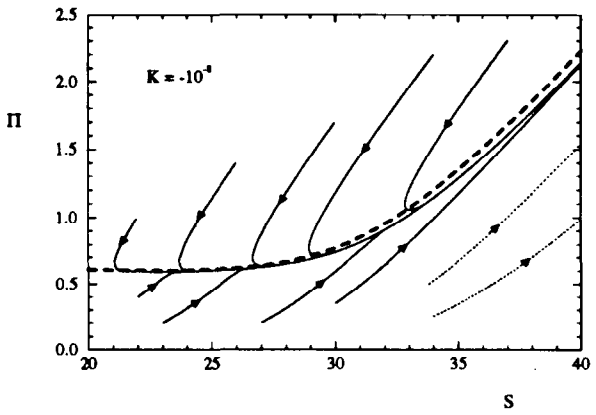

Figure 8: Source flow calculations for $K = \nu/(LU_0) = -10^{-8}$. Heavy broken line is the quasi-equilibrium solution of Perry et al.[1].

3.2.2 Zero pressure gradient flow

In figure 9 is shown the case of a zero pressure gradient flow calculated using closure equation (16) in conjunction with (8). The evolution equations were solved for three different initial conditions, including Coles' standard trip condition. These solutions rapidly approach the quasi-equilibrium solution of Perry et al.[1], which is also shown in figure 9. Coles[15] suggests Π can be correlated with R_θ, for a given initial condition and provides a curve fit for the so called 'standard trip initial condition'. Using (9) such a relationship can also be expressed on the $\Pi - S$ phase plane and this is shown by the heavy line in figure 9. It can be seen the Coles curve fit approaches the quasi-equilibrium solution more gradually than the solution computed using (16) and starting from the same standard trip initial condition. This highlights the tentative nature of (16), being based on very sparse data and in order to get better agreement with experiments further high quality experiments are required to formulate (16).

It is important to note that the current formulation implies that a zero pressure gradient layer is not an equilibrium layer but it is an autonomous layer which rapidly asymptotes into a quasi-equilibrium layer and does reach a state of precise equilibrium (self-similarity) only at infinite Reynolds numbers.

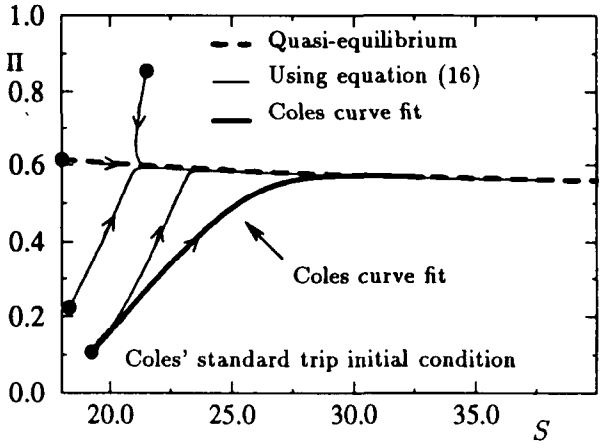

Figure 9: Zero pressure gradient flow showing; quasi-equilibrium calculation of Perry et al.[1] and current calculation using (16) with various initial conditions also shown is the Coles[15] curve fit.

3.2.3 Approaching sink flow

A recent thorough study of sink flows was carried out by Jones[4] and these are also considered here. Such flows are a good example of favourable pressure gradient flows. A sink flow turbulent boundary layer is one whose pressure gradient follows that of a two-dimensional potential sink. The flow is shown schematically in figure 10. Townsend[16] and Rotta[17] identified sink flow as the only smooth wall boundary layer that may evolve to a state of precise equilibrium at finite S for flows which are two-dimensional in the mean. A precise equilibrium layer is one where all mean and turbulence measurements are invariant with the streamwise direction, when they are scaled with the correct velocity and length scale.

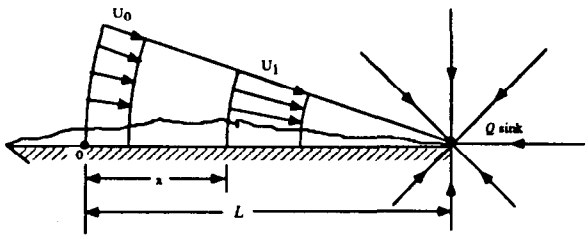

Figure 10: Schematic of sink flow boundary layer, note origin for x is arbitrary.

In this experimental study, three acceleration parameters (K) were investigated with a total of 62 mean-flow stations. Figure 11 shows the corresponding β_a versus Π data. Expression (16) is not expected to apply in this range of Π.

The heavy solid line shown in figure 11 corresponds to a curve fit for the $\zeta_a = 0$ data points with the functional form

$$\beta_{ae} = -0.5 + 1.38\Pi + 0.13\Pi^2. \qquad (22)$$

Equations (22) and (19) are very close for Π greater than about 2. The lines of constant ζ_a shown in figure 11 come from a localised surface fit:

$$\zeta_a = (0.85 - 6.9\Pi + 8\Pi^2)\Delta\beta_a \qquad (23)$$

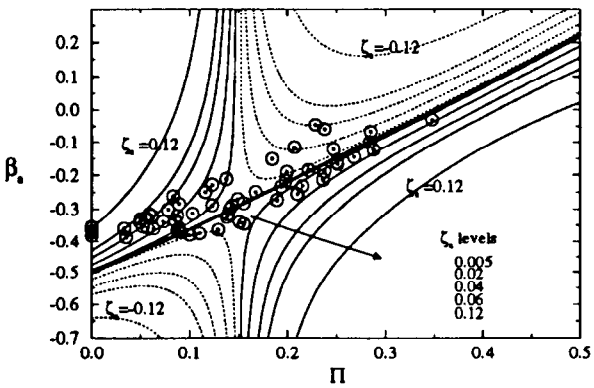

Figure 11: Data of Jones[4]. Each point has a different value of ζ_a. Solid line corresponds to equation (22) for $\zeta_a = 0$.

Using (23), (13) and the least-squares-error shear-stress profile matching, formulation (4) can be described and thus equations (10) and (11) can now be used to compute the evolution of the boundary layer given any initial station where Π, S, β and ζ are known. Figure 12 show a comparison between the experimental data and computation and good agreement is observed. This shows that the closure scheme is a viable one and indicates that the mathematical machinery is working correctly.

4 Conclusions and Discussion

A framework has been constructed for formulating closure for a turbulent boundary layer evolving in an arbitrary streamwise pressure gradient. This involves using the well known mean-flow scaling laws such as Prandtl's law of the wall and the law of the wake of Coles together with the mean continuity and the mean momentum differential and integral equations. The important parameters governing the flow are identified from the shear stress formulation derived by Perry et al.[1]. The Reynolds shear stress profiles are assumed to form a two parameter family as opposed to a one parameter family implied in many eddy viscosity models.

Evolution equations based on an integral approach are consistent with the attached eddy hypothesis which utilises convolution integrals. The above approach seems more reasonable physically than most differential field methods because in reality, the transport properties at one point in the flow must be intimately related to motions remote from that point. This feature is an important aspect of the attached eddy hypothesis.

Initially closure is done here semi-empirically from experimental data and using the wall-wake attached eddy model of Perry and Marusic[10]. Comparisons are made with experiments covering adverse pressure gradient flows in relaxing and developing states and flows approaching equilibrium sink flow and reasonably good agreement is observed.

The proposed formulations for $\psi[\Pi, \beta_a, \zeta_a]$ are very tentative and the variation between its form between adverse and favourable pressure gradient flows gives some idea of the complexity that may be involved in one general formulation covering all flows. The aim of the present work was to describe the appropriate framework and assess its viability. The viability of the scheme has been demonstrated here and further experimental data would be needed so that a single formulation covering a broad range of parameters can be developed. The use of models such as those based on the attached eddy hypothesis show potential and should with further development be useful in helping map out the $\Pi - \beta_a - \zeta_a$ space with appropriate interpolation and extrapolation schemes. Once the mean flow development can be calculated the attached eddy model of Perry and Marusic[10] could be used to evaluate the relevant turbulence quantities, such as Reynolds stresses and spectra.

The authors wish to acknowledge the financial assistance of the Australian Research Council.

Appendix

$$R = \frac{S}{\kappa S^2 C_1 - \kappa S C_2 + C_2} + \frac{\beta(2SC_1 - C_2)}{C_1(\kappa S^2 C_1 - \kappa S C_2 + C_2)} + \frac{\zeta(dC_2/d\Pi - S dC_1/d\Pi - N(C_2 - SC_1))}{\kappa S^2 C_1 - \kappa S C_2 + C_2},$$

where

$$N = W_c[1, \Pi] + \Pi \frac{dW_c[1, \Pi]}{d\Pi},$$

and using (9) $N = 2$,

$$C_1[\Pi] = \int_0^\infty \frac{U_1 - U}{U_\tau} d\eta,$$

$$C_2[\Pi] = \int_0^\infty (\frac{U_1 - U}{U_\tau})^2 d\eta,$$

$$E[\Pi] = \exp\left[-\kappa\left(A + \frac{\Pi}{\kappa} W_c[1, \Pi]\right)\right],$$

References

[1] A. E. Perry, I. Marusic, and J. D. Li. Wall turbulence closure based on classical similarity laws and the attached eddy hypothesis. *Phys. Fluids*, 6 (2):1024–1035, 1994.

[2] D. E. Coles. The law of the wake in the turbulent boundary layer. *J. Fluid Mech.*, 1:191–226, 1956.

[3] I. Marusic and A. E. Perry. A wall-wake model for the turbulence structure of boundary layers. part 2. further experimental support. *J. Fluid Mech.*, 298:389–407, 1995.

[4] M. B. Jones. *Evolution and structure of sink-flow turbulent boundary layers.* PhD thesis, University of Melbourne, Australia, 1998.

[5] L. F. East, W. G. Sawyer, and C. R. Nash, 1979. An investigation of the structure of equilibrium turbulent boundary layers. *R.A.E. Tech Report* 79040.

[6] A. E. Perry, I. Marusic, and M. B. Jones. New evolution equations for turbulent boundary layers in arbitrary pressure gradients. In *Proc. 7th Asian Congress of Fluid Mechanics*, Chenai, India, 1997. Also *Sadhana*, Indian Academy of Sci. To appear, 1998.

[7] A. K. Lewkowicz. An improved universal wake function for turbulent boundary layers and some of its consequences. *Z. Flugwiss. Weltraumforsch.*, 6:261–266, 1982.

[8] P. Bradshaw and D. Ferriss. The response of a retarded equilibrium boundary layer to the sudden removal of pressure gradient. Technical Report 1145, NPL Aero. Report, 1965.

[9] A. E. Samuel and P. N. Joubert. A boundary layer developing in an increasingly adverse pressure gradient. *J. Fluid Mech.*, 66: 481–505, 1974.

[10] A. E. Perry and I. Marusic. A wall-wake model for the turbulence structure of boundary layers. part 1. extension of the attached eddy hypothesis. *J. Fluid Mech.*, 298:361–388, 1995.

[11] F. M. White. *Viscous Fluid Flow.* McGraw-Hill, New York., 1974.

[12] P. E. Skåre and P.-Å. Krogstad. A turbulent boundary layer near separation. *J. Fluid Mech.*, 272:319–348, 1994.

[13] F. H. Clauser. Turbulent boundary layers in adverse pressure gradients. *J. Aero. Sci.*, 21: 91–108, 1954.

[14] I. Marusic. *The structure of zero- and adverse- pressure gradient turbulent boundary layers.* PhD thesis, University of Melbourne, Australia, 1991.

[15] D. E. Coles, 1962. The turbulent boundary layer in a compressible fluid. *USAF The Rand Cooperation, Rep. R-403-PR*, Appendix A.

[16] A. A. Townsend. *The structure of turbulent shear flow.* 1st. edn. Cambridge University Press, 1956.

[17] J. C. Rotta. Turbulent boundary layers in incompressible flow. *Prog. Aero. Sci.*, 2:1–219, 1962.

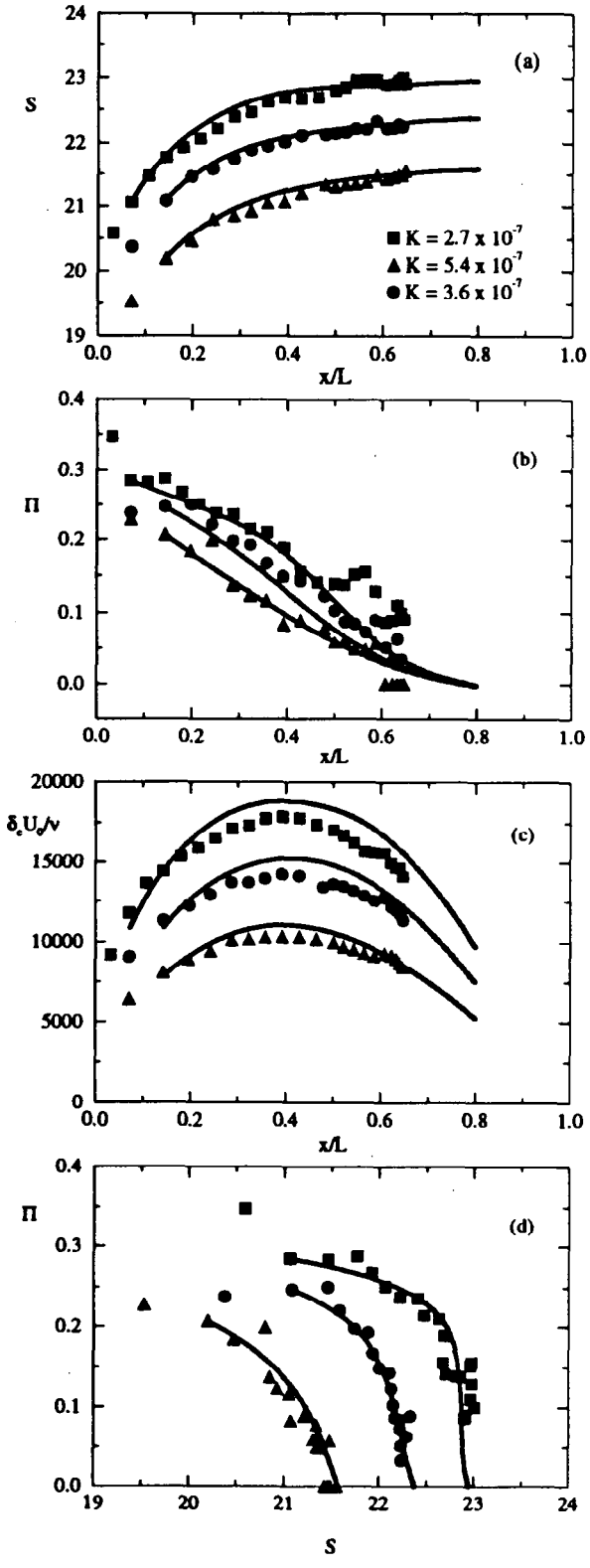

Figure 12: Evolution of mean flow parameters for flow of Jones (1998). Symbols represent data; solid lines correspond to calculation. Note in these figures x is measured from the trip wire.